Proc. Natl. Acad. Sci. USA
Vol. 92, pp. 9235–9239, September 1995
Neurobiology

Impairment of synaptic vesicle clustering and of synaptic transmission, and increased seizure propensity, in synapsin I-deficient mice

LIAN LI*†, LIH-SHEN CHIN*, OLEG SHUPLIAKOV‡, LENNART BRODIN‡, TALVINDER S. SIHRA§, ØIVIND HVALBY¶, VIDAR JENSEN¶, DAKE ZHENG‖, JAMES O. MCNAMARA‖**, PAUL GREENGARD*, AND PER ANDERSEN¶

*Laboratory of Molecular and Cellular Neuroscience, The Rockefeller University, New York, NY 10021; ‡Department of Neuroscience, Karolinska Institutet, S-171 77 Stockholm, Sweden; §Department of Pharmacology, Royal Free Hospital School of Medicine, University of London, Rowland Hill Street, London, NW3 2PF, United Kingdom; ¶Department of Neurophysiology, University of Oslo, N-0317 Oslo, Norway; Departments of ‖Medicine (Neurology) and of **Neurobiology and Pharmacology, Duke University Medical Center and Durham Veterans Affairs Medical Center, Durham, NC 27710

Contributed by Per Andersen, June 13, 1995

ABSTRACT **Synapsin I has been proposed to be involved in the modulation of neurotransmitter release by controlling the availability of synaptic vesicles for exocytosis. To further understand the role of synapsin I in the function of adult nerve terminals, we studied synapsin I-deficient mice generated by homologous recombination. The organization of synaptic vesicles at presynaptic terminals of synapsin I-deficient mice was markedly altered: densely packed vesicles were only present in a narrow rim at active zones, whereas the majority of vesicles were dispersed throughout the terminal area. This was in contrast to the organized vesicle clusters present in terminals of wild-type animals. Release of glutamate from nerve endings, induced by K^+, 4-aminopyridine, or a Ca^{2+} ionophore, was markedly decreased in synapsin I mutant mice. The recovery of synaptic transmission after depletion of neurotransmitter by high-frequency stimulation was greatly delayed. Finally, synapsin I-deficient mice exhibited a strikingly increased response to electrical stimulation, as measured by electrographic and behavioral seizures. These results provide strong support for the hypothesis that synapsin I plays a key role in the regulation of nerve terminal function in mature synapses.**

A great deal of evidence has implicated the synapsins in the regulation of synaptogenesis and in the modulation of neurotransmitter release from adult nerve terminals (1–4). To further assess the possible roles of synapsin I in the regulation of these processes, we have generated synapsin I-deficient mice by homologous recombination. In an accompanying paper (5), we report that axonal outgrowth and synaptogenesis are severely impaired in these mutant mice. Herein we present evidence that synapses of the adult synapsin I mutant mice manifest a variety of structural and physiological abnormalities.

MATERIALS AND METHODS

Synapsin I-Deficient Mice. Synapsin I mutant mice were generated by homologous recombination (5). Littermates of wild-type and synapsin I mutant mice were used in all of the analyses. Only male mice were used to avoid any variation caused by the estrous cycle of female mice. Except for glutamate release assays, all analyses were carried out by investigators without any knowledge of the genotype of the animal.

Electron Microscopy. Wild-type (n = 2) and synapsin I-deficient mice (n = 3) were anesthetized with pentobarbital (40 mg/kg; i.p.) and perfused transcardially with Tyrode's solution followed by 3% (vol/vol) glutaraldehyde/0.5% paraformaldehyde in 0.1 M sodium phosphate-buffered saline (pH 7.4). Spinal cords and brains were dissected and postfixed in the same fixative for 4 h. Segments L4 and L5 of the spinal cord were cut into 60- to 100-μm transverse sections and hippocampi were cut into longitudinal sections. The sections were postfixed in 1% osmium tetroxide, dehydrated in alcohol, and embedded in Durcupan. Semithin (1 μm) and ultrathin ("silver") sections were cut from the tissue blocks on an ultratome. The semithin sections were mounted on glass slides and counterstained with cresyl violet for light microscopic analysis. The ultrathin sections were mounted on Formvar-coated copper grids, counterstained with uranyl acetate and lead citrate, and examined in a Philips CM12 electron microscope. To compare the structural organization of synapses between the two groups of animals, we focused on one well-defined class of terminal in the intermediate gray matter and dorsal part of the ventral horn (laminae V–VII) of the spinal cord. This type of terminal, referred to as the "S-type terminal" (6), has a diameter of <4 μm, contains spherical synaptic vesicles, and forms asymmetric synapses with the soma and dendrites of spinal neurons. It contains high levels of glutamate (O.S. and S. Cullheim, unpublished data).

All terminals of this type encountered during random screening of the intermediate gray matter and dorsal part of the ventral horn were included, provided that they exhibited distinct synaptic specializations. The screening was continued in each animal until a sample of 30 terminals had been collected. The density of synaptic vesicles and the length of the active zone were quantified from electron micrographs (×39,000 and ×51,000) with a digitizing tablet coupled to a computer using MORFOREL software (7).

Preparation of Synaptosomes and Assay of Glutamate Release. Synaptosomes from the cerebral cortex (male mice, 2–3 months of age) were purified on Percoll gradients as described (8) with minor modifications (9). Glutamate release was assayed by on-line fluorimetry as described (10, 11). Glutamate release was monitored by measuring the increase of fluorescence due to the production of NADPH, which is generated from the reduction of $NADP^+$ by the oxidative deamination of released glutamate catalyzed by glutamate dehydrogenase (12).

Electrophysiological Analyses in the Hippocampus. In transverse hippocampal slices (nine from mutant and eight from wild-type mice), Schaffer collateral-commissural fibers were stimulated at high frequency for 1 min to deplete the neurotransmitter content of the boutons. Before and after the tetanizing period, the synapses were tested every 6 sec. The amplitude and initial slope of field excitatory postsynaptic potential (f-EPSP) were recorded from the apical dendrites of

The publication costs of this article were defrayed in part by page charge payment. This article must therefore be hereby marked "*advertisement*" in accordance with 18 U.S.C. §1734 solely to indicate this fact.

Abbreviations: 4AP, 4-aminopyridine; f-EPSP, field excitatory postsynaptic potential.

†To whom reprint requests should be addressed.

CA1 pyramidal cells. In addition to the experimental (tetanized) pathway, a set of control fibers, terminating on the basal dendrites of the same neurons (control pathway), was stimulated every 6 sec (alternating with stimulation to the tetanized pathway) to monitor neurotransmission at nondepleted synapses of the same type. These experiments were performed in 50 μM D-(−)-2-amino-5-phosphonopentanoate (AP5, Sigma) to avoid interference arising from the induction of long-term potentiation after tetanus. The size of the presynaptic volley was monitored to ensure that a constant number of afferent fibers were stimulated with each test volley.

In a separate set of experiments, long-term potentiation was evoked in CA1 pyramidal neurons by established techniques (13), in slices maintained in artificial cerebrospinal fluid without added AP5. The initial slope and amplitude of f-EPSPs were compared in control and synapsin I-deficient mice.

Preparation of Mice for Evaluation of Seizure Propensity. Five wild-type and seven homozygous null mutant mice at least 4 months of age underwent stereotaxic implantation of a bipolar stimulating–recording electrode in the right amygdala under pentobarbital anesthesia (50–60 mg/kg) by using the following coordinates with bregma as a reference: 0.7 mm posterior; 2.8 mm lateral; 4.5 mm below dura. A ground electrode was placed in the skull overlying the left frontal cortex. After a postoperative recovery period of at least 1 week, a 1-sec train of 60-Hz/1.0-msec biphasic rectangular pulses at a current intensity of 60 μA was administered. Subsequent trains of increasing current intensity (by 20 μA) with 1-min intervals were given until an electrographic seizure of at least 5 sec was observed. The behavioral manifestations of seizures were classified by a modification of Racine (14) as follows: 1, chewing; 2, head nodding; 3, unilateral forelimb clonus; 4, bilateral forelimb clonus; 5, bilateral forelimb clonus plus falling and/or hindlimb clonus; 6, running or bouncing seizure. After the completion of the experiment, electrode placement was verified as described (15).

RESULTS

Clustering of Synaptic Vesicles at Release Sites Is Impaired in Synapsin I-Deficient Mice. Light microscopic analysis of Nissl-stained sections from brain and spinal cord did not reveal any obvious structural differences between control and synapsin I-deficient mice (data not shown), in agreement with the study of Rosahl *et al.* (16).

Ultrastructural analysis of sections from hippocampus and spinal cord showed that synaptic vesicles of normal size and shape accumulated at active zones of synapses in both wild-type and mutant mice. However, while distinct clusters of vesicles were present at active zones in wild-type animals, no dense vesicle clusters were apparent in the terminals of mutant mice. To obtain an objective measure of the clustering of vesicles, one defined population of glutamatergic synapses in the spinal cord known to contain comparatively large vesicle clusters (S-type terminals) was selected for quantitative analysis. In wild-type animals, these terminals contained prominent clusters of densely packed synaptic vesicles at active zones (Fig. 1), but in the mutant mice the organization of vesicles was altered. Thus, only a narrow rim of densely packed vesicles were present at the active zones (Fig. 1 *B* and *C*), and the majority of the vesicles were dispersed throughout the cross-sectional area of the terminals. Quantitative analysis showed that the density of vesicles within a distance of 150 nm from the active zone was similar between the two groups of animals, while the density in the vesicle-containing area located 150–500 nm from the active zone was significantly lower ($P < 0.001$) in synapsin I-deficient mice compared to wild-type mice (Fig. 2). The length of the active zone, the terminal area, the total number of synaptic vesicles per terminal, and the density of vesicles in the whole terminal area were similar between wild-type and synapsin I-deficient mice.

Decreased Neurotransmitter Release in Synaptosomes from Synapse I-Deficient Mice. Disruption of the synapsin I gene resulted in a decrease in 4-aminopyridine (4AP)-, KCl-, and ionomycin-induced release of glutamate from mutant mice, compared to their wild-type littermates (Fig. 3). There was no significant difference in the 4AP- or KCl-evoked Ca^{2+}-independent release of glutamate from wild-type and mutant mouse synaptosomes (data not shown), indicating that the decrease in release seen with the synapsin I mutants was

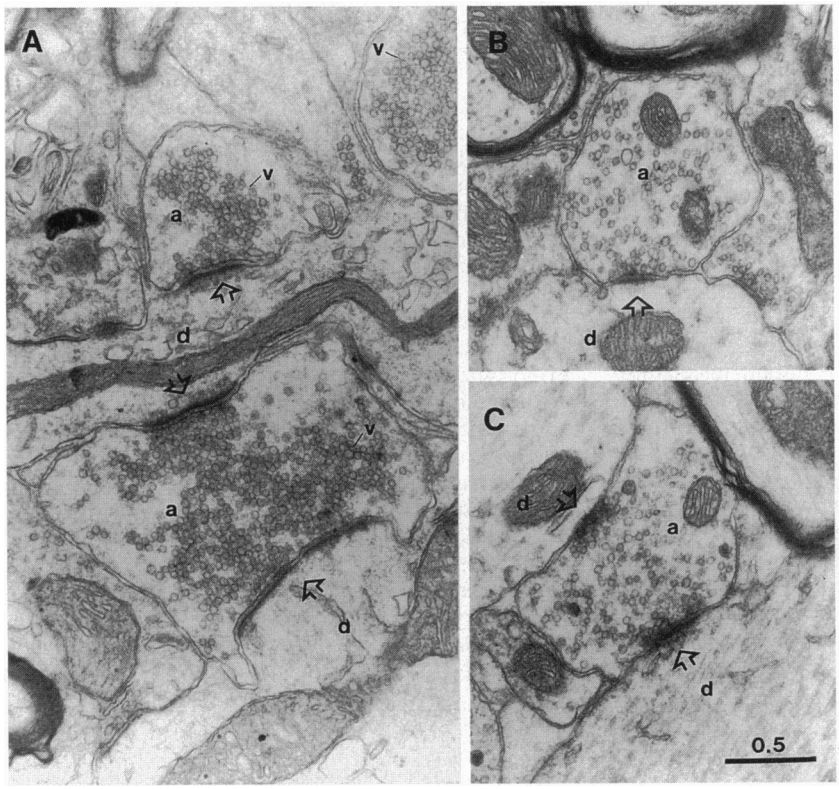

FIG. 1. Altered synaptic vesicle clustering in synapsin I-deficient mice. (*A*) Electron micrograph of axon terminals (a) that establish asymmetrical synapses on dendrites (d) of spinal neurons in a wild-type mouse. (*B* and *C*) Axon terminals of the same type from synapsin I-deficient mice. Note the presence of compact vesicle clusters (v) in the terminals of the wild-type mouse that are lacking in the mutant mice. Arrows indicate active zones. (Bar = 0.5 μm.)

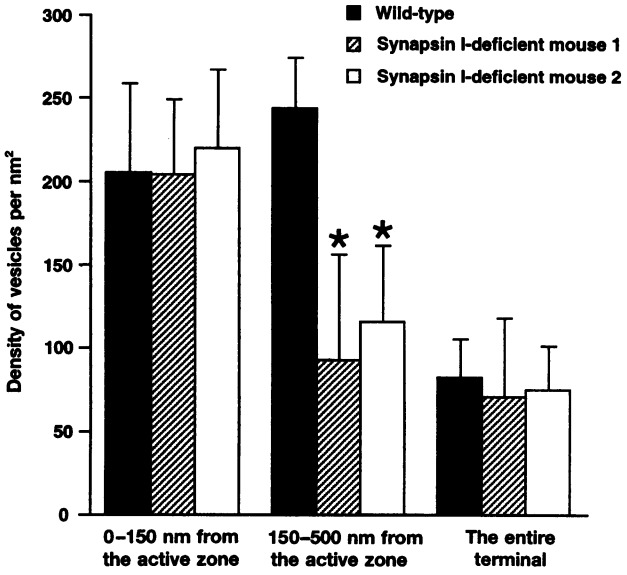

FIG. 2. Quantitative comparison of the density of synaptic vesicles in excitatory terminals of wild-type and synapsin I-deficient mice. Solid bars represent mean values (±SD) from 30 terminals in a wild-type mouse. The hatched and open bars represent corresponding values for 30 terminals from two mutant mice. *, Statistically significant differences between control and mutant mice ($P < 0.001$). Mean length of the active zones in studied profiles was 1.1 ± 0.4 nm in the wild-type mouse and 1.0 ± 0.5 nm and 1.1 ± 0.4 nm (±SD) in the two mutant mice.

attributable to alteration of a vesicular event leading to exocytosis (10).

Delayed Recovery of Synaptic Transmission in Synapsin I-Deficient Mice After Tetanic Stimulation. High-frequency stimulation caused a rapid reduction in the amplitude of the f-EPSPs and a short-lasting depression of the presynaptic volley (Fig. 4 *A–C*). During the tetanus, the f-EPSP was reduced to zero by a 100-Hz stimulation (Fig. 4 *A–C*) and to 4% by a 20-Hz stimulation (data not shown), in both wild-type ($n = 8$) and mutant ($n = 9$) mice.

After both 20-Hz (Fig. 4 *D* and *E*) and 100-Hz stimulation frequencies (duration, 1 min), the f-EPSP recovered to a pretetanus level in two phases. The first recovery phase after the 20-Hz tetanus had time constants of 1.3 ± 0.2 min and 1.4 ± 0.3 min ($P > 0.1$) for slices from wild-type and mutant animals, respectively. This initial component was followed by a much slower second phase that was significantly prolonged in slices from mutant mice, lasting 11.3 ± 4.3 min (mean ± SD) in wild-type mice ($n = 8$) and 28.6 ± 6.2 min in mutant mice ($n = 9$) (Fig. 3 *D–F*). Examples of recovery of synaptic transmission are shown for two individual slices, one from a wild-type mouse (Fig. 3*D*) and one from a mutant mouse (Fig. 3*E*), to indicate the method used for measuring the recovery time. The difference in time to recovery was highly significant ($P < 0.00001$, Student's *t* test). Fitting of a straight line or an exponential curve to this tail gave nearly identical results. After the 100-Hz stimulation, the recovery times were also significantly different ($P < 0.03$) between slices from wild-type (8.9 ± 5.0 min) and synapsin I-deficient (23.8 ± 5.1 min) mice. The recovery time was not significantly changed by increasing the duration of the 100-Hz stimulation to 10 min.

Analysis of the nontetanized control pathways revealed that the tetanic stimulation led to a general depression with an exponential recovery roughly corresponding to the initial phase of recovery of the tetanized pathway. This depression is probably due to a postsynaptic conductance increase arising from the intense synaptic bombardment and was not statistically different between the two animal groups in either magnitude or duration ($P > 0.2$). The first phase of the recovery is likely to reflect this general depression, because it expressed itself to the same degree and with a similar time course in the control pathways in both animal groups. In contrast, the slow recovery phase of CA1 synaptic potentials could reflect the depletion of vesicles or transmitter or the slowed replenishment of transmitter in the distal pool of vesicles. This replenishment seems necessary for high-frequency transmitter release, because it clearly outlasted the transient reduction of both the presynaptic volley and the control recovery period.

LTP and Post-Tetanic Potentiation Are Not Altered in Synapsin I-Deficient Mice. No significant differences in LTP were found in hippocampal slices of synapsin I-deficient mice compared to wild-type mice, in agreement with Rosahl *et al.* (16). The amount of enhancement, measured 30 min after induction (100 Hz for 1 sec), was 34 ± 8% for the mutants and 32 ± 7% for the wild-type animals. Slices from both types of animal also showed a similar amount and time course of post-tetanic potentiation (data not shown).

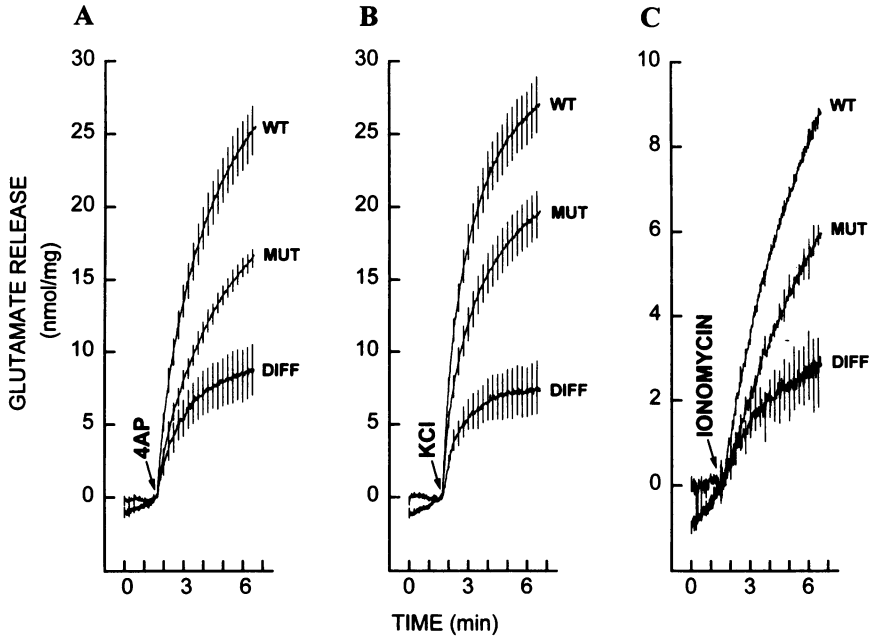

FIG. 3. Glutamate release from synaptosomes from wild-type and synapsin I-deficient mice. Glutamate release was evoked by the addition of 3 mM 4AP (*A*), 30 mM KCl (*B*), or 10 μM ionomycin (*C*) in the presence of 1 mM Ca^{2+}. Traces: WT, release from synaptosomes from wild-type mice; MUT, release from synapsin I-deficient littermates; DIFF, difference between the two. Each trace is the mean of eight (*A* and *B*) or four (*C*) experiments. Bars represent the SEM.

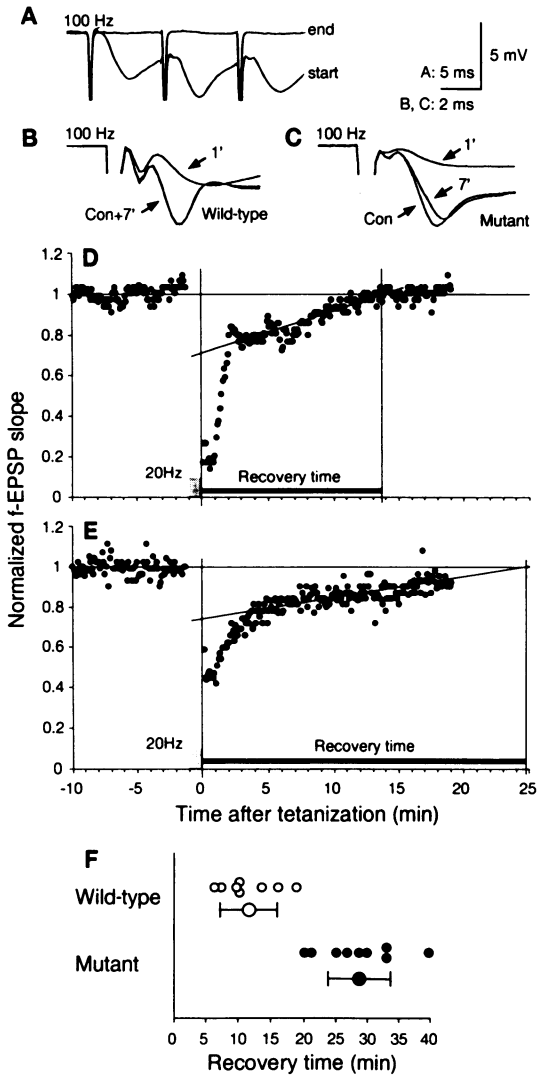

FIG. 4. Delayed recovery of hippocampal CA1 synaptic transmission in synapsin I-deficient mice after high-frequency stimulation. (*A*) Sample records of CA1 synaptic responses during the 100-Hz stimulation of afferent fibers in the stratum radiatum of wild-type mouse. The first three responses of the 1-min tetanus are marked start, and the last three are marked end. (*B*) Average of five responses to low-frequency activation (0.17 Hz) of CA1 synapses in wild-type mice, taken before (Con) and 1 and 7 min after cessation of the 100-Hz stimulation for 1 min (traces were superimposed). The control and 7-min responses overlap completely. The 1-min record shows post-tetanic depression. (*C*) Same protocol as *B* but in a slice from a mutant mouse. Note that the 7-min response has still not fully recovered. (*D*) Normalized f-EPSP slope of radiatum/CA1 synapses in a slice taken from a wild-type mouse, showing the two-phased recovery after stimulation at 20 Hz for 1 min (shaded box). The oblique line is a linear regression through the data points collected through the slow recovery phase (starting 4 min after the end of the tetanus). (*E*) Similar to *D* but in a slice from a mutant mouse. (*F*) Graph showing the recovery times for wild-type ($n = 8$, ○) and mutant ($n = 9$, ●) mice. The large circles and horizontal lines give the respective means and standard deviations ($P < 0.00001$).

Stimulation-Evoked Epileptic Seizures Are Enhanced in Synapsin I-Deficient Mice. The response to a brief low-intensity electrical stimulation through an electrode in the amygdala disclosed a striking increase in excitability of synapsin I mutant mice. A small normally subconvulsive electrical stimulus of the right amygdala of wild-type mice typically induced a short electrographic seizure [Fig. 5*A*; duration 11.7 ± 1.3 sec (mean ± SEM), $n = 5$]. These electrographic seizures ordinarily occurred without overt behavioral manifestations. In contrast, an equivalent stimulus of synapsin I-deficient mice evoked electrographic seizures (Fig. 5*B*) of longer duration (22.5 ± 2.8 sec, $n = 7$), exceeding that of wild-type littermates by 92% (Student's t test, $P < 0.01$). The increased duration of electrographic seizures in synapsin I-deficient mice was accompanied by striking behavioral seizures, typically consisting of generalized clonic motor activity. The intensity of behavioral seizures was 0.6 ± 0.4 for wild-type and 3.9 ± 0.8 for synapsin I-deficient mice (mean ± SEM, $P < 0.01$). In contrast to the enhanced responses to electrical stimulation, no significant differences were found in the current intensity required to evoke a seizure (172 ± 26 μA for wild-type vs. 146 ± 15 μA for synapsin I mutant mice).

DISCUSSION

The impaired clustering of synaptic vesicles in synapsin I-deficient mice indicates that synapsin I regulates the organization of a large portion of the synaptic vesicle cluster at release sites. A smaller portion of the vesicles located adjacent to the active zone did appear to be normal in synapsin I-deficient mice. This suggests that synaptic vesicles form two distinct pools, of which one, but not the other, depends on synapsin I for its organization. In a study of giant synapses in lamprey (17), a similar distinction between synapsin-dependent and synapsin-independent pools of vesicles was found: immunocytochemistry revealed a selective localization of synapsin to the distal part of synaptic vesicle clusters, and injection of synapsin antibodies into the living presynaptic element caused a selective depletion of the distal part of the cluster. Moreover, it is interesting to note that ribbon synapses in the retina, which lack synapsins (18), do not contain conventional synaptic vesicle clusters, but rather a narrow rim of vesicles tethered to the presynaptic structure (19, 20). The ultrastructural studies of vesicle clusters, together with the physiological results described above, suggest that the distal pool of vesicles is not required for low-frequency neurotransmitter release but that it is necessary for stable high-frequency release.

The mechanism underlying the increased paired pulse facilitation in synapsin I-deficient mice (16) has not been elucidated. Moreover, it cannot be reliably determined in mutant animals due to the alterations in the structure and function of synapses. The increased facilitation may not be due to an alteration in the facilitation mechanism *per se*. It may result, at least in part, from a reduced initial synaptic potential (due to reduced neurotransmitter release) leading to a greater relative increase in the second synaptic potential. Alternatively, since synaptic vesicles can act as calcium buffers (21), the increased facilitation may be due to the decreased vesicle density resulting in an impaired calcium buffering in the vicinity of active zones.

The striking intensity of both electrographic and behavioral seizures evoked by a tiny electrical stimulation of the amygdala of synapsin I-deficient mice demonstrates that synapsin I regulates the excitability of populations of neurons *in situ*. The cause of this hyperexcitability is unclear. The delayed synapse formation evident in hippocampal neurons isolated from the mutant mice (5) raises the possibility of abnormal development of synaptic connectivity *in situ*. Alternatively, the absence of synapsin I in the mature brain could underlie the increased excitability. The synapsin I mutant mice exhibit defects in synaptic function, as shown by the demonstrated reduction of synaptosomal glutamate release and delayed recovery of synaptic responses of CA1 pyramidal cells after tetanic activation of their excitatory afferents. Synapsin I-deficient mice also show a dramatic decrease in release of γ-aminobutyric acid from nerve terminals in slices of neostriatum (J.-A. Girault, L.L., L.-S.C., F. Artaud, A. Cheramy, and P.G., unpublished data). The heightened seizure responses evident *in situ* suggest

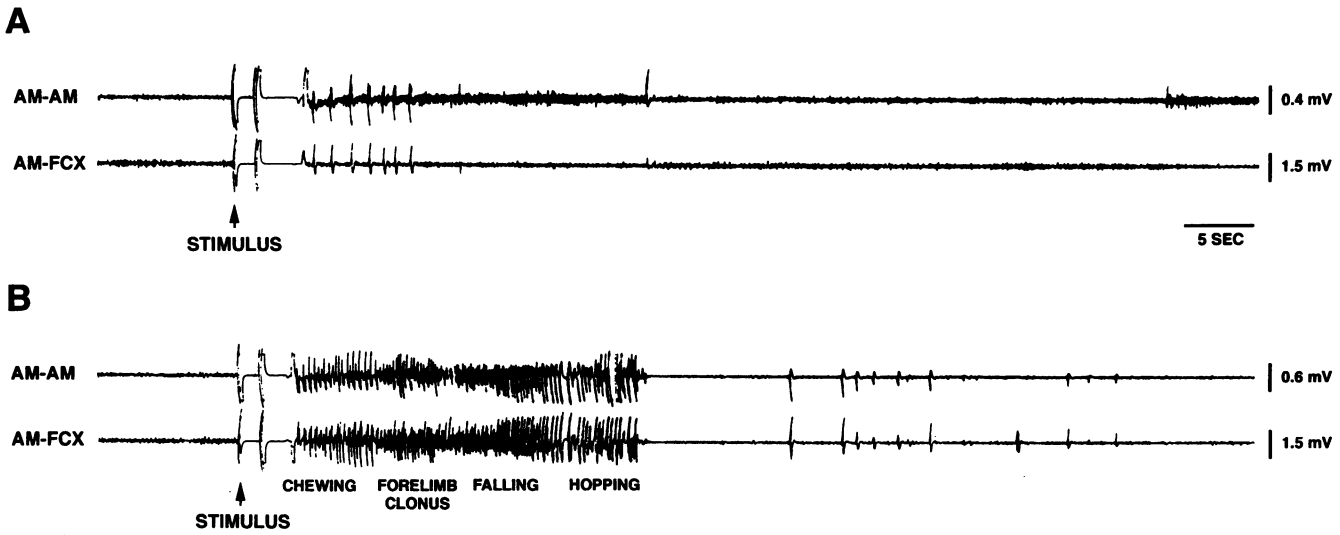

FIG. 5. Representative electroencephalogram after an electrical stimulus of wild-type and synapsin I-deficient mice. (*A*) In a wild-type mouse, an electrographic seizure of 13 sec was recorded from the bipolar electrode in the right amygdala (trace AM-AM) and between electrodes in right amygdala and overlying left frontal cortex (trace AM–FCX) after an amygdala stimulation of 220 μA. No obvious behavioral seizure was observed. (*B*) A synapsin I-deficient mouse exhibited an electrographic seizure of 28 sec and a class 5 seizure after a stimulation of 200 μA.

that the normal delicate balance between inhibitory and excitatory synaptic transmission is shifted in favor of net hyperexcitability in the synapsin I mutant mice.

CONCLUDING REMARKS

This study has revealed prominent alterations in the structure and function of synapses in synapsin I-deficient mice. At the behavioral level, the functional abnormality was manifested as an increased susceptibility to seizures. Although these data demonstrate a role for synapsin I in synaptic function, it is possible that the effect of the mutation underestimates the significance of synapsin I in the adult brain. As synapses are highly plastic, it seems likely that functional deficits become partly masked by compensatory changes.

Finally, the results of the studies presented here, and in the accompanying papers (4, 5), provide direct evidence that synapsin I plays a major role both in the regulation of neuronal development and in the regulation of synaptic function in the adult animal. It will be of importance to determine whether synapsin I achieves these two distinct categories of effect through similar mechanisms.

We thank Ms. L. Butler for excellent technical assistance, Drs. A. Fienberg and V. Pieribone for valuable help and advice, and Ms. L. Mandel for assistance in preparation of this manuscript. This work was supported by U.S. Public Health Service Grants MH39327 (P.G.) and NS17771 and NS32334 (J.O.M.), by the Swedish Medical Research Council MFR11287 (L.B.), and by a U.K. Wellcome Trust University Award (T.S.S.).

1. Greengard, P., Valtorta, F., Czernik, A. J. & Benfenati, F. (1993) *Science* **259,** 780–785.
2. Schaeffer, E., Alder, J., Greengard, P. & Poo, M.-m. (1994) *Proc. Natl. Acad. Sci. USA* **91,** 3882–3886.
3. Ferreira, A., Kosik, K. S., Greengard, P. & Han, H.-Q. (1994) *Science* **264,** 977–979.
4. Ferreira, A., Han, H.-Q., Greengard, P. & Kosik, K. S. (1995) *Proc. Natl. Acad. Sci. USA* **92,** 9225–9229.
5. Chin, L.-S., Li, L., Ferreira, A., Kosik, K. S. & Greengard, P. (1995) *Proc. Natl. Acad. Sci. USA* **92,** 9230–9234.
6. Conradi, S. (1969) *Acta Physiol. Scand. Suppl.* **332,** 5–48.
7. Blackstad, T. W., Karagulle, T. & Ottersen, O. P. (1990) *Comput. Biol. Med.* **20,** 15–34.
8. Dunkley, P. R., Jarvie, P. E., Heath, J. W., Kidd, G. J. & Rostas, J. A. P. (1986) *Brain Res.* **372,** 115–129.
9. Wang, J. K. T., Walaas, S. I., Sihra, T. S., Aderem, A. & Greengard, P. (1989) *Proc. Natl. Acad. Sci. USA* **86,** 2253–2256.
10. Nicholls, D. G. & Sihra, T. S. (1986) *Nature (London)* **321,** 772–773.
11. Sihra, T. S., Bogonez, E. & Nicholls, D. G. (1992) *J. Biol. Chem.* **267,** 1983–1989.
12. Greengard, P. (1956) *Nature (London)* **178,** 632–634.
13. Malenka, R. C., Kauer, J. A., Zucker, R. S. & Nicoll, R. A. (1988) *Science* **242,** 81–84.
14. Racine, R. J. (1972) *Electroencephalogr. Clin. Neurophysiol.* **32,** 281–294.
15. McNamara, J. O., Galloway, M. T., Rigsbee, L. C. & Shin, C. (1984) *J. Neurosci.* **4,** 2410–2417.
16. Rosahl, T. W., Geppert, M., Spillane, D., Herz, J., Hammer, R. E., Malenka, R. C. & Südhof, T. C. (1993) *Cell* **75,** 661–670.
17. Pieribone, V. A., Shupliakov, O., Brodin, L., Hilfiker-Rothenfluh, S., Czernik, A. J. & Greengard, P. (1995) *Nature (London)* **375,** 493–497.
18. Mandell, J. W., Townes-Anderson, E., Czernik, A. J., Cameron, R., Greengard, P. & De Camilli, P. (1990) *Neuron* **5,** 19–33.
19. Usukura, J. & Yamada, E. (1987) *Cell Tissue Res.* **247,** 483–488.
20. Dowling, J. E. (1987) *The Retina: An Approachable Part of the Brain* (Harvard Univ. Press, Cambridge, MA).
21. Bower, J. M. & Haberly, L. B. (1986) *Proc. Natl. Acad. Sci. USA* **83,** 1115–1119.